Inorganica Chimica Acta, 28 (1978) 159–168

Electronic Spectra of Some Tetragonal Complexes of Rhodium(III), Iridium(III) and Platinum(IV) [1]

WILLIAM D. BLANCHARD and W. ROY MASON*

Department of Chemistry, Northern Illinois University, DeKalb, Ill. 60115, U.S.A.

Received September 19, 1977

Solution electronic spectral data are reported for 30 tetragonal complexes of the types trans-$M(en)_2X_2^{n+}$, $M(NH_3)_5X^{n+}$ *(M = Rh(III), Ir(III), or Pt(IV); X = Cl, Br, or I);* trans-$M(NH_3)_4X_2^{n+}$ *(M = Rh(III) or Pt(IV); X = Cl, Br, or I);* trans-$PtL_4X_2^{2-}$ *(L = CN^- or NO_2^-, X = Cl or Br); and* $Pt(CN)_5X^{2-}$ *(X = Cl, Br, or I). These data are interpreted in terms of ligand field (LF) excited states in* C_{4v} *or* D_{4h} *symmetry and ligand to metal charge transfer (LMCT) excited states involving the halide ligands. Intensity patterns among the LMCT transitions of intermediate intensity are rationalized by including halide spin–orbit coupling in excited configurations. Trends in LF and LMCT excited state energies are discussed.*

Introduction

Electronic spectra have provided an important experimental basis for the development of electronic structural models for low spin octahedral ML_6^n complexes (O_h symmetry) of nd^6 metal ions [2, 3]. The details of these models now seem clear and in many cases fairly complete spectral interpretation is available [4–7]. In contrast, electronic spectra of tetragonal complexes of the type ML_5X^n (C_{4v} symmetry) or *trans*-$ML_4X_2^m$ (D_{4h} symmetry) are not so well understood, even though the extension of octahedral models to these lower symmetries is straightforward [8]. This is especially true for spectra of tetragonal complexes of the 2nd and 3rd row metal ions Rh(III), Ir(III) and Pt(IV), where data [9–19] have been widely scattered, incomplete, and in a few cases, suspect because of the presence of interfering counterions, hydrolysis or photolysis. Spectral interpretation, where available, often has been incomplete or lacking in detail, particularly for the intense charge-transfer bands exhibited by many of these complexes [2, 5, 9–11]. Also, many of the complexes of the nd^6 metal ions are photochemically active [20, 21]. Therefore an understanding of the nature of low lying excited states is of interest in devising potentially useful photosynthetic reactions [22, 23]. Accordingly we have systematically collected spectral data under carefully controlled conditions for 30 tetragonal complexes of the following type: *trans*-$M(en)_2X_2^{n+}$, $M(NH_3)_5X^{m+}$ (M = Rh(III), Ir(III), or Pt(IV); X = Cl, Br, or I), *trans*-$M(NH_3)_4X_2^{n+}$ (M = Rh(III) or Pt(IV); X = Cl, Br, or I), *trans*-$PtL_4X_2^{2-}$ (L = CN^- or NO_2^-; X = Cl or Br), and $Pt(CN)_5X^{2-}$ (X = Cl, Br, or I). In many cases our spectral measurements have extended data beyond what was previously available, and new bands have been identified and assigned. In addition to ligand field band assignments, a detailed interpretation of charge-transfer spectra, including the effects of ligand spin–orbit coupling, is also presented.

Experimental

The complexes investigated are all known complexes and their syntheses have been described in the literature [12–14, 16, 24–34]. Nitrate or halide salts of $Rh(NH_3)_5X^{2+}$ [13, 24], $Ir(NH_3)_5X^{2+}$ [25], *trans*-$Rh(en)_2X_2^+$ [13], *trans*-$Rh(NH_3)_4X_2^+$ [12c, 13] and *trans*-$Ir(en)_2X_2^+$ [14] (X = Cl, Br, or I) were converted to perchlorate salts by precipitation from concentrated aqueous solutions with 72% perchloric acid at ice bath temperatures. Suspensions of the less soluble halide salts of *trans*-$Pt(en)_2X_2^{2+}$ [16, 26] or *trans*-$Pt(NH_3)_4X_2^{2+}$ [27] were first treated with stoichiometric amounts of silver perchlorate and the silver halide removed before precipitating the cationic complexes with 72% perchloric acid at ice bath temperature. Phosphate salts of $Pt(NH_3)_5Cl^{3+}$ and $Pt(NH_3)_5Br^{3+}$ [28] and the carbonate salt of $Pt(NH_3)_5I^{3+}$ [29] were converted to perchlorate salts by dissolving in dilute perchloric acid and precipitating with ice cold 72% perchloric acid. Tetraethylammonium salts of $Pt(CN)_5X^{2-}$ or $Pt(CN)_4X_2^{2-}$ were precipitated from concentration aqueous solutions of the potassium salts [30–33] by the addition of a concentrated aqueous solution of $(C_2H_5)_4NX$. Published methods [33, 34] were used to prepare $K_2[Pt(NO_2)_4Cl_2]$ and $K_2[Pt(NO_2)_4Br_2]$. The compounds used for spectral measurements all gave satisfactory elemental analyses.

*To whom correspondence should be addressed.

Electronic spectral measurements were obtained using a Cary 1501 spectrophotometer. Spectral grade acetonitrile was used for solutions of the tetraethylammonium salts. Some low temperature spectra for selected compounds were obtained using a Cryo-Tip hydrogen refrigerator (Air Products and Chemicals, Inc.); temperatures below 100 K were measured with a calibrated gallium arsenide diode. Low temperature measurements were made on thin solid films of polyvinyl alcohol (PVA) containing water soluble compounds or of methylmethacrylate containing alkyl ammonium salts soluble in dichloromethane. The details of the film preparation have been described elsewhere [35].

Results and Discussion

Molecular Orbitals and Excited States

Simplified one-electron molecular orbital energy level diagrams for the C_{4v} ML_5X^n and D_{4h} *trans*-$ML_4X_2^m$ tetragonal complexes are given in Figures 1 and 2. Since the electron configuration of the metal ions is $4d^6$ or $5d^6$, the highest filled levels are 3e and $2e_g$ respectively. The ground states are diamagnetic and totally symmetric, designated $^1A_1$ and $^1A_{1g}$.

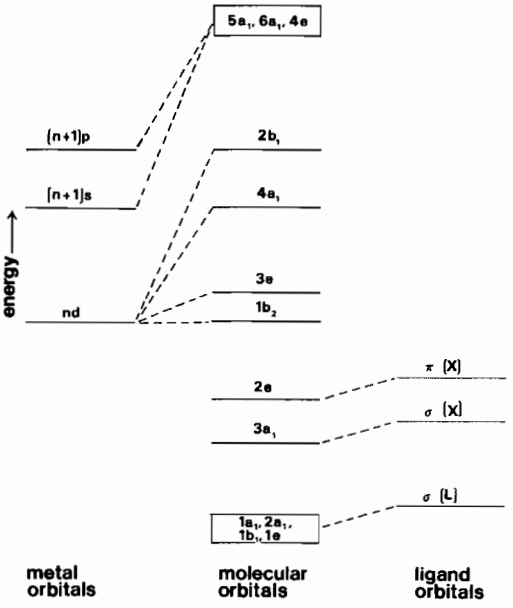

Fig. 1. Molecular orbital energy levels for a C_{4v} ML_5X^n complex.

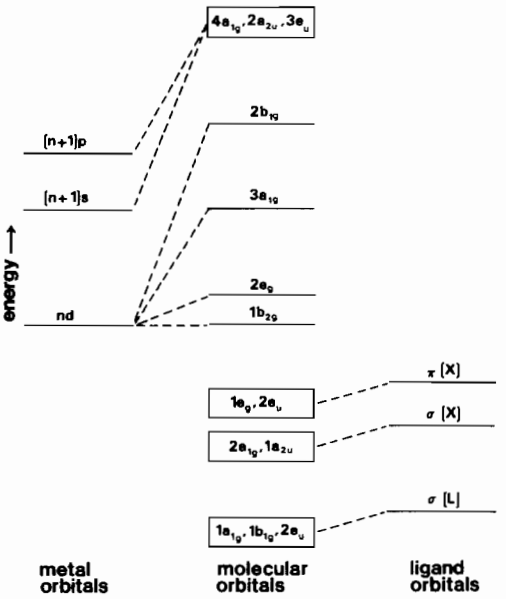

Fig. 2. Molecular orbital energy levels for a D_{4h} *trans*-$ML_4X_2^m$ complex.

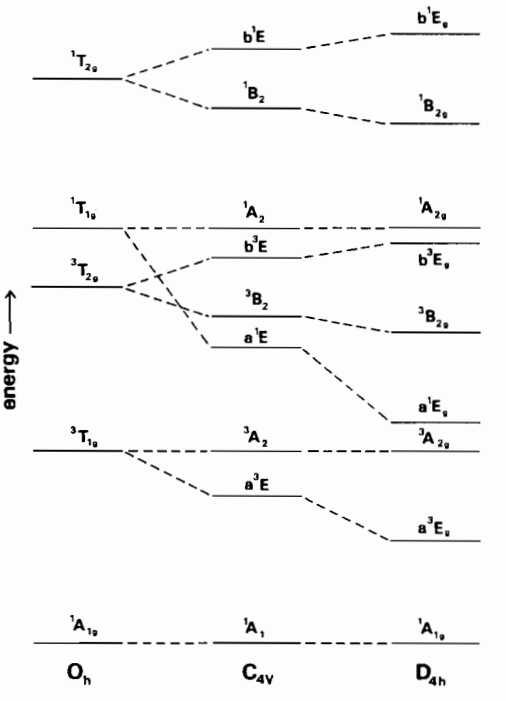

Fig. 3. Correlation of ligand field states between octahedral symmetry and C_{4v} or D_{4h} symmetry.

Low energy electronic excited states for these halogen containing complexes can be divided into two types. The first are ligand field (LF) states resulting from transitions from occupied MO's of mainly *n*d character ($1b_2$ or 3e and $1b_{2g}$ or $2e_g$) to the lowest energy empty orbitals ($4a_1$ or $2b_1$ and $3a_{1g}$ or $2b_{1g}$) also predominantly *n*d in character. The second are ligand to metal charge-transfer (LMCT) states resulting from transitions from halide based MO's ($3a_1$ or 2e and $1a_{2u}$ or $2e_u$) to the empty *n*d orbitals of the metal.

The LF excited states expected for the C_{4v} and D_{4h} complexes can be easily correlated with those of octahedral complexes as shown in Figure 3 [8, 36].

For all the complexes investigated the halide ligands X lie lower in the spectrochemical series than the ligands L. Therefore the a^1E or a^1E_g state derived from $^1T_{1g}$ will be lower in energy than $^1A_2$ or $^1A_{2g}$, which is expected to be nearly the same energy as $^1T_{1g}$ in the ML_6^n complex [36]. The splitting of the states derived from $^1T_{2g}$ is predicted to be smaller than those from $^1T_{1g}$, and in practice for a variety of tetragonal Co(III) complexes [36] transitions to these states have not been resolved. The intensities of transitions to the singlet LF states are expected to be low in keeping with the predominantly metal d orbital character of the MO's involved. Intensities of spin-forbidden LF transitions are expected to be even lower but increase with metal spin–orbit coupling which allows relaxation of spin selection rules by admixture of spin-allowed states. The free ion value for the spin–orbit coupling constant ζ_{4d} for Rh(III) is *ca.* 1400 cm^{-1}, while ζ_{5d} for Ir(III) or Pt(IV) is estimated to be in the range 4000–5000 cm^{-1} [5]. Therefore spin forbidden LF transitions will be relatively more intense for Ir(III) and Pt(IV) complexes than for Rh(III) complexes.

The LMCT excited states in the absence of spin–orbit coupling include $^{1,3}E$, $^{1,3}A_1$ and $^{1,3}B_1$ states for the C_{4v} complexes and $^{1,3}E_u$, $^{1,3}A_{2u}$ and $^{1,3}B_{2u}$ states for the D_{4h} complexes ($^{1,3}E_g$ and $^{1,3}A_{2g}$ states can also be visualized for the D_{4h} complexes but transitions to these states are parity forbidden and are expected to be weak and obscured by the more intense bands at similar energies). If halogen spin–orbit coupling is included, transitions to LMCT states which are formally triplet states, can gain intensity by coupling with allowed singlet states. The magnitude of the coupling is determined by ζ_{np} for the halogen, for which free atom values are 587 cm^{-1}, 2457 cm^{-1} and 5069 cm^{-1} for Cl, Br and I respectively [37]. Table I lists the spin–orbit states for the excited LMCT configurations of the C_{4v} and D_{4h} complexes; the symbols for the spin–orbit states are characterized by the lack of spin-multiplicity superscripts. Of all the spin–orbit states possible for these configurations only transitions to the E and A_1 or E_u and A_{2u} states will be allowed by dipole selection rules, and then in proportion to the ^1E and $^1A_1$ or ^1E_u and $^1A_{2u}$ character in the spin–orbit eigenvectors. Secular determinants for evaluating spin–orbit eigenvectors and eigenvalues are given in Table II, where the diagonal elements contain the energies of the singlet and triplet states in the absence of spin–orbit interaction and ζ is the halide *n*p spin–orbit coupling constant in the complex. The determinant elements were determined by approximating the MO's of the LMCT states as pure metal *n*d or halide *n*p atomic orbitals and neglecting terms involving more than one center. Metal centered integrals are zero so spin–orbit coupling is limited to the halide alone. Furthermore there is no mixing between the excited configurations

TABLE I. Excited Configurations and Symmetry Representations of Excited States.

Excited Configuration[a]	Excited States (No Spin–Orbit Coupling)	Spin–Orbit States
C_{4v} Complexes		
$(2e)^3(4a_1)$	^1E	E
	^3E	E, A_1, A_2, B_1, B_2
$(3a_1)(4a_1)$	$^1A_1$	A_1
	$^3A_1$	E, A_2
$(2e)^3(2b_1)$	^1E	E
	^3E	E, A_1, A_2, B_1, B_2
$(3a_1)(2b_1)$	$^1B_1$	B_1
	$^3B_1$	E, B_2
D_{4h} Complexes[b]		
$(2e_u)^3(3a_{1g})$	^1E_u	E_u
	^3E_u	$E_u, A_{1u}, A_{2u}, B_{1u}, B_{2u}$
$(1a_{2u})(3a_{1g})$	$^1A_{2u}$	A_{2u}
	$^3A_{2u}$	E_u, A_{1u}
$(2e_u)^3(2b_{1g})$	^1E_u	E_u
	^3E_u	$E_u, A_{1u}, A_{2u}, B_{1u}, B_{2u}$
$(1a_{2u})(2b_{1g})$	$^1B_{2u}$	B_{2u}
	$^3B_{2u}$	E_u, B_{1u}

[a]See Figures 1 and 2. [b]Parity forbidden states involving excitations from $2a_{1g}$ or $1e_g$ omitted.

TABLE II. Spin–Orbit Secular Determinants for LMCT States.[a]

C_{4v} Complexes	D_{4h} Complexes
A_1 states ($X \rightarrow 4a_1$)	A_{2u} states ($X \rightarrow 3a_{1g}$)
$\begin{vmatrix} {}^1A_1 - E & +\zeta/2^{1/2} \\ \zeta/2^{1/2} & {}^3E - \zeta/2 - E \end{vmatrix}$	$\begin{vmatrix} {}^1A_{2u} - E & +\zeta/2^{1/2} \\ +\zeta/2^{1/2} & {}^3E_u - \zeta/2 - E \end{vmatrix}$
E states ($X \rightarrow 4a_1$)	E_u states ($X \rightarrow 3a_{1g}$)
$\begin{vmatrix} {}^3A_1 - E & \mp\zeta/2 & +i\zeta/2 \\ \mp\zeta/2 & {}^1E - E & \pm i\zeta/2 \\ -i\zeta/2 & \mp i\zeta/2 & {}^3E - E \end{vmatrix}$	$\begin{vmatrix} {}^3A_{2u} - E & \mp\zeta/2 & +i\zeta/2 \\ \mp\zeta/2 & {}^1E_u - E & \pm i\zeta/2 \\ -i\zeta/2 & \mp i\zeta/2 & {}^3E_u - E \end{vmatrix}$
E states ($X \rightarrow 2b_1$)	E_u states ($X \rightarrow 2b_{1g}$)
$\begin{vmatrix} {}^3B_1 - E & \mp\zeta/2 & +i\zeta/2 \\ \mp\zeta/2 & {}^1E - E & \pm i\zeta/2 \\ -i\zeta/2 & \mp i\zeta/2 & {}^3E - E \end{vmatrix}$	$\begin{vmatrix} {}^3B_{2u} - E & \mp\zeta/2 & +i\zeta/2 \\ \mp\zeta/2 & {}^1E_u - E & \pm i\zeta/2 \\ -i\zeta/2 & \mp\zeta/2 & {}^3E_u - E \end{vmatrix}$

[a]The elements of the 3×3 determinants are phase dependent, and although the choice of phase is arbitrary, care must be taken to be internally consistent. The "±" signs included here refer to two equivalent choices of phase.

involving the metal d_{z^2} orbital ($4a_1$ or $3a_{1g}$) and those involving the metal $d_{x^2-y^2}$ orbital ($2b_1$ or $2b_{1g}$).

Electronic Spectra

Solution spectral data obtained at room temperature are collected in Table III. Where our measurements overlap with previous reports [9–19] and where hydrolysis, photolysis, or absorbing counterions can be excluded in the previous investigations, the agreement is generally satisfactory. In addition to the room temperature solution measurements of Table III several low temperature (22–25 K) measurements on selected complexes in solid PVA or methylmethacrylate films were made to determine the temperature dependence of bands of intermediate intensity. Figure 4, which typifies the results obtained, shows the spectra at 300 K and 22 K for the 4.35 μm^{-1} band of *trans*-$[Ir(en)_2Br_2]ClO_4$. The changes in the spectra of the solid films as a function of temperature were completely reversible.

Spectral Assignments

The lower energy, lower intensity bands ($\epsilon < 400$) observed in the spectra of the Rh(III), Ir(III) and Pt(IV) complexes are logically assigned as LF transitions. The energies of corresponding bands vary with the halide ligand I < Br < Cl in a manner predicted by the spectrochemical series. The more intense bands ($\epsilon > 2000$) at higher energy are assigned as LMCT. Consistent with this assignment, the energies of corresponding transitions parallel metal orbital stability and are observed in the order Rh(III) < Ir(III) > Pt(IV) for complexes of the same structural type. Bands are also observed which have intermediate intensities ($\epsilon \sim 400$–1500). These bands are more difficult to assign since they may be visualized either as LF transitions enhanced in intensity by coupling to adjacent allowed transitions or to weak LMCT transitions which might be formally spin or orbitally forbidden. Band assignments for individual complexes are included in Table III, and their rationale will be discussed in turn.

TABLE III. Electronic Spectral Data.[a]

Band No.	$\bar{\nu}$, μm^{-1} (ϵ, M^{-1} cm^{-1})			Excited State[b]
	X = Cl	X = Br	X = I	
trans-$[Rh(en)_2X_2]ClO_4$				
I	2.47(80.4)	2.36(116)	2.17(266)	a^1E_g
II	3.48(120)			b^1E_g, $^1B_{2g}$
III	4.13(1,600)[c]	3.63(2900)	2.97(14,500)	$^{1,3}E_u[(2e_u)^3(3a_{1g})]$
IV	4.86(39,000)	4.30(37,000)	3.72(34,000)	$^1A_{2u}[(1a_{2u})(3a_{1g})]$
V			4.55(11,000)[c]	$^{1,3}E_u[(2e_u)^3(2b_{1g})]$
VI			4.92(16,000)	I^- intralig.
trans-$[Rh(NH_3)_4X_2]ClO_4$				
I	2.44(72.5)	2.32(136)	2.14(304)	a^1E_g
II	3.45(91.0)			b^1E_g, $^1B_{2g}$
III		3.68(3,800)	2.97(15,000)	$^{1,3}E_u[(2e_u)^3(3a_{1g})]$
IV	4.81(33,000)	4.27(39,000)	3.72(28,000)	$^1A_{2u}[(1a_{2u})(3a_{1g})]$
V			4.84(19,000)	I^- intralig.
trans-$[Ir(en)_2X_2]ClO_4$				
I	2.40(7)	2.25(9)	2.03(12)	a^3E_g
II	2.92(48)	2.76(68)	2.53(165)	a^1E_g
III	3.60(35)[c]	3.46(30)		$^1A_{2g}$ or triplet LF
IV		4.35(3,280)[c]	3.56(13,800)	$^{1,3}E_u[(2e_u)^3(3a_{1g})]$
V			4.36(43,000)	$^1A_{2u}[(1a_{2u})(3a_{1g})]$
VI			4.95(16,300)[c]	I^- intralig.
trans-$[Pt(en)_2X_2](ClO_4)_2$				
I	2.70(20)[c]	2.35(20)[c]		a^3E_g
II	3.03(101)	2.70(172)[c]		a^1E_g
III	3.81(920)	3.13(1,150)		$^{1,3}E_u[(2e_u)^3(3a_{1g})]$
IV	4.82(34,500)	4,25(35,000)		$^1A_{2u}[(1a_{2u})(3a_{1g})]$

TABLE III *(Continued)*

Band No.	$\bar{\nu}$, μm^{-1} (ϵ, M^{-1} cm^{-1})			Excited State[b]
	X = Cl	X = Br	X = I	
trans-$[Pt(NH_3)_4X_2](ClO_4)_2$				
I	2.66(18)[c]	2.32(19)[c]	1.80(51)	a^3E_g
II	2.99(91.4)	2.67(175)		a^1E_g
III	3.86(560)	3.16(1200)	2.60(2400)[d]	$^{1,3}E_u[(2e_u)^3(3a_{1g})]$
IV	4.80(31,000)	4.24(32,000)	3.60(1600)[d]	$^1A_{2u}[(1a_{2u})(3a_{1g})]$
V			4.39(3600)[d]	$^{1,3}E_u[(2e_u)^3(2b_{1g})]$
$[Rh(NH_3)_5X](ClO_4)_2$[e]				
I		2.35(24)[c]		a^3E
II	2.90(101)	2.80(124)	2.42(286)	a^1E
III			2.60(250)[c]	$^1A_2$ or triplet LF
IV	3.64(109)			b^1E, $^1B_2$
V		4.15(1060)[c]	3.62(3400)	$^{1,3}[(2e)^3(4a_1)]$
VI	5.32(29,000)[c]	4.92(29,000)	4.44(30,000)	$^1A_1[(3a_1)(4a_1)]$
$[Ir(NH_3)_5X](ClO_4)_2$[e]				
I	2.76(9.5)[c]	f	f	a^3E
II	3.49(72)	3.31(84)	2.99(360)	a^1E
III	4.42(370)			b^1E, $^1B_2$
IV		4.38(760)	4.29(4500)	$^{1,3}E[(2e)^3(4a_1)]$
V	5.07(1780)[c]	4.85(3100)[c]	4.65(6,600)	$^{1,3}E[(2e)^3(2b_1)]$
VI			5.24(35.000)	$^1A_1[(3a_1)(4a_1)]$
$[Pt(NH_3)_5X](ClO_4)_3$[e]				
I	3.54(180)	3.11(256)	2.58(840)	a^1E
II			2.87(610)[c]	$^1A_2$ or triplet LF
III			3.60(4200)[c]	$^{1,3}E[(2e)^3(4a_1)]$
IV		4.96(23,400)	4.20(10,800)	$^1A_1[(3a_1)(4a_1)]$
V			5.00(16,600)	I^- intralig.
$[(C_2H_5)_4N]_2[Pt(CN)_5X]$[g]				
I	3.84(222)			a^1E
II		3.42(588)	3.04(2420)	$^{1,3}E[(2e)^3(4a_1)]$
III	5.14(29,400)	4.90(37,700)	4.55(38.000)	$^1A_1[(3a_1)(4a_1)]$
IV			4.95(13,000)	I^- intralig.
$[(C_2H_5)_4N]_2[Pt(CN)_4X_2]$[g]				
I	2.65(30)[c]	2.30(39)[c]		a^3E_g
II	3.05(180)[c]			a^1E_g
III	3.47(450)	2.88(1370)		$^{1,3}E_u[(2e_u)^3(3a_{1g})]$
IV	4.58(35,700)	4.14(47,700)		$^1A_{2u}[(1a_{2u})(3a_{1g})]$
$K_2[Pt(NO_2)_4X_2]$				
I	3.05(7680)	3.05(7470)[c]		NO_2^- intralig.
II	3.61(21,600)	3.61(21,350)		NO_2^- intralig.
III		4.33(27,100)		$^1A_{2u}[(1a_{2u})(3a_{1g})]$
IV	5.10(37,800)	5.10(32,800)		NO_2^- intralig.

[a]Aqueous solution, room temperature. [b]Excited state configuration given for LMCT transitions (filled orbitals omitted); orbitals labeled as in Figure 1 or Figure 2. [c]Shoulder, ϵ is for the value of $\bar{\nu}$ given. [d]Beer's law not obeyed; solution concentration = 9.4×10^{-5} *M*. [e]0.010 *M* $HClO_4$ solution. [f]Shoulders at 2.6(10) and 2.4(14) μm^{-1} reported in ref. 9 for $Ir(NH_3)_5Br^{2+}$ and $Ir(NH_3)_5I^{2+}$, respectively, could not be located, even though a careful search was made using concentrated solutions. [g]Acetonitrile solution.

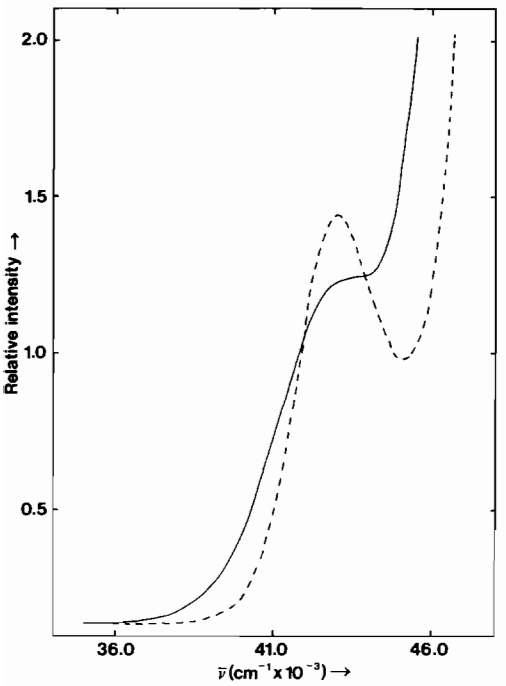

Fig. 4. Absorption spectrum of *trans*-$[Ir(en)_2Br_2]ClO_4$ in a solid polyvinylalcohol film. ——, 300 K, – – –, 22 K.

Trans-*M(en)*$_2X_2^n$ *and* trans-*M(NH*$_3$*)*$_4X^n$ *Complexes*

The LF bands observed for these complexes were interpreted using the scheme in Figure 3. Only the transition to a ^1E_g is observed in each case. In addition to the expected spectrochemical ordering of the transition energies, a systematic increase in band intensity is also observed in the order Cl < Br < I. This pattern likely reflects the diminishing energy difference between allowed LMCT states at higher energy and the LF a^1E_g state, resulting in enhanced vibronic intensity stealing by the LF transition. The Ir(III) and Pt(IV) complexes exhibit a weak band lower in energy than the $^1A_{1g} \rightarrow a^1E_g$ transition. This weak band is assigned as $^1A_{1g} \rightarrow a^3E_g$. For the Rh(III) complexes where the metal spin–orbit coupling is substantially lower, this transition is expected to be weaker and therefore is not resolved at room temperature. A low temperature (80 K) study [38] of *trans*-$[Rh(en)_2Cl_2]Cl$ in glassy solution showed some evidence of a weak shoulder at 2.13 μm^{-1} ($\epsilon \sim 1.5$), which is probably due to the $^1A_{1g} \rightarrow a^3E_g$ transition.

The spectra of *trans*-$Rh(en)_2Cl_2^+$, *trans*-$Rh(NH_3)_4Cl_2^+$, *trans*-$Ir(en)_2Cl_2^+$, and *trans*-$Ir(en)_2Br_2^+$ each reveal an additional higher energy LF band. The band in the Rh(III) complexes (band II) is higher in energy than the $^1A_{1g} \rightarrow {}^1T_{1g}$ transition in $Rh(en)_3^{3+}$ (3.32 μm^{-1}) or $Rh(NH_3)_6^{3+}$ (3.27 μm^{-1}) [10], and therefore may be reasonably assigned as the unresolved transitions to the $^1B_{2g} + b^1E_g$ states, which derive from the $^1T_{2g}$ O_h state. In contrast the band observed for the Ir(III) complexes (band III) lies *lower* in energy than the $^1A_{1g} \rightarrow {}^1T_{1g}$ transition in $Ir(en)_3^{3+}$ (4.02 μm^{-1}) [10] and thus excludes an assignment to $^1B_{2g} + b^1E_g$. A possible assignment for band III, consistent with its relatively lower intensity, is a transition to the equatorially localized $^1A_{2g}$ state. However, this assignment implies the $^1A_{2g}$ state is substantially lower in energy than the $^1T_{1g}$ state in $Ir(en)_3^{3+}$. Such a situation is difficult to rationalize in terms of LF or simple MO theory. An alternative assignment of band III might be as one or more transitions to spin-forbidden LF states which are expected between a^1E_g and $^1A_{2g}$ (see Figure 3). The band intensity can be rationalized by noting that the strong metal spin–orbit coupling present in Ir(III) complexes will cause considerable mixing of the spin-allowed and spin-forbidden LF states, especially if the energy differences between them in the absence of coupling are not very large. For example, the E_g spin–orbit component of $^3B_{2g}$ will mix with a^1E_g. If these two states are reasonably close in energy, as they are expected to be, then mixing will be quite large giving considerable singlet character to the spin-forbidden transition. Additional experimental work is needed to resolve this question, and a polarized single crystal measurement is planned.

The relatively intense bands which are prominent in the spectra of the *trans*-$M(en)_2X_2^n$ and *trans*-$M(NH_3)_4X_2^n$ complexes are assigned to LMCT transitions. These transitions may be divided into two types: σ-LMCT which involve the occupied σ orbital of X, $1a_{2u}$ and π-LMCT which involve the occupied π orbitals of X, $2e_u$. Straightforward theoretical considerations, together with established experimental patterns for LMCT bands in a wide variety of halide complexes [2–4, 7, 39] lead to the expectation that for a given empty acceptor orbital on the metal allowed π-LMCT transitions will lie at lower energy and will be less intense than the σ-LMCT transition. Thus for LMCT to the lowest energy virtual orbital $3a_{1g}(d_{z^2})$ the transition to $^1A_{2u}$ ($1a_{2u} \rightarrow 3a_{1g}$) should be more intense and lie at higher energy than the transition to ^1E_u ($2e_u \rightarrow 3a_{1g}$). The LMCT excitations to the $2b_{1g}$ ($d_{x^2-y^2}$) orbital are expected at higher energy. In thise case, the σ-LMCT transition ($1a_{2u} \rightarrow 2b_{1g}$) gives rise to an orbitally forbidden $^1B_{2u}$ excited state and therefore will be very weak and obscured by more intense allowed transitions. The π-LMCT transition ($2e_u \rightarrow 2b_{1g}$) will give rise to an allowed ^1E_u state, but transitions to this state are expected to be less intense than the $^1A_{1g} \rightarrow {}^1A_{2u}$ σ-LMCT. Consequently the most intense LMCT band in the spectra of the *trans*-$M(en)_2X_2^n$ and *trans*-$M(NH_3)_4X_2^n$ complexes (band IV, except for $Ir(en)_2X_2^+$, where the band in question is band V) is assigned as $^1A_{1g} \rightarrow {}^1A_{2u}$.

A less intense band, lower in energy than $^1A_{1g} \rightarrow {}^1A_{2u}$ is observed in each case except for *trans*-$Ir(en)_2Cl_2^+$ and is assigned to the π-LMCT to $3a_{1g}$ (d_{z^2}). The intensity of this band (band III for Rh(III) and Pt(IV), for Ir(III) band IV) is a marked function of

the halide ligand with the observed order Cl < Br < I. For example the relative absorptivities of band III for the *trans*-$Rh(en)_2X_2^+$ complexes are 1:1.8:9.1 for X = Cl, Br, and I respectively. This order of intensities parallels the magnitude of ζ_{np} for the halide ligand and thus suggests that spin-forbidden LMCT bands are present which are weak for X = Cl but gain intensity by strong mixing with allowed states for X = I. Therefore, to provide guidance in the interpretation of the observed intensity patterns and to gain insight into the nature of the LMCT excited states involved, some simple spin–orbit calculations were performed. A similar approach to the intensities in the LMCT spectra of $Co(NH_3)_5X^{2+}$ was described by Yamatera [40]. These calculations involve diagonalizing the appropriate spin–orbit secular determinants (Table II) using input energies for the singlet and triplet states in the absence of spin–orbit coupling, together with the halide spin–orbit coupling constant. The choice of input energies for the ^1E_u, ^3E_u, $^1A_{2u}$, and $^3A_{2u}$ states was guided by the band energies observed in the experimental spectra. The energy differences between ^1E_u and ^3E_u or $^1A_{2u}$ and $^3A_{2u}$ were assumed to be small, however. The calculations were not very sensitive to the exact size of these energy differences. Values of ζ_{np} for the halides in the complexes were arbitrarily reduced to 80% of the free atom values to allow for covalency. Table IV presents the results of a typical set of calculations,

TABLE IV. Calculated Spin–Orbit States for *trans*-$Rh(en)_2X_2^+$.

State	Calculated Energy, μm^{-1} (% singlet character)[a]		
	X = Cl[b]	X = Br[c]	X = I[d]
$E_u(^3A_{2u})$	4.83(0)	4.27(3)	3.71(15)
$E_u(^1E_u)$	4.13(89)	3.89(62)	3.55(50)
$E_u(^3E_u)$	4.05(11)	3.66(36)	3.00(35)
$A_{2u}(^1A_{2u})$	4.87(100)	4.31(96)	3.73(82)
$A_{2u}(^3E_u)$	4.04(0)	3.63(4)	2.98(18)

[a]From squared coefficient of $|^1E_u>$ or $|^1A_{2u}>$ in normalized spin–orbit eigenvector. [b]Input energies (in μm^{-1}): ζ_{3p} = 0.47, $^1A_{2u}$ = 4.87, $^3A_{2u}$ = 4.83, ^1E_u = 4.12, ^3E_u = 4.06. [c]Input energies (in μm^{-1}): ζ_{4p} = 0.20, $^1A_{2u}$ = 4.28, $^3A_{2u}$ = 4.24, ^1E_u = 3.82, ^3E_u = 3.76. [d]Input energies (in μm^{-1}): ζ_{5p} = 0.41, $^1A_{2u}$ = 3.60, $^3A_{2u}$ = 3.56, ^1E_u = 3.38, ^3E_u = 3.32.

in this case for the *trans*-$Rh(en)_2X_2^+$ complexes. It is clear from these results that the singlet character in the A_{2u} and E_u components of ^3E_u increase substantially as the size of halide ligand is increased. In view of the relative intensities expected for the allowed $^1A_{1g} \rightarrow {}^1A_{2u}$ and $^1A_{1g} \rightarrow {}^1E_u$ transitions, the calculations indicate that the primary contribution to the increase in band intensity is due to $^1A_{2u}$ character in the A_{2u} component of ^3E_u, with a secondary contribution from ^1E_u in the E_u component. Since only a single band is observed in the experimental spectra the A_{2u} and E_u spin–orbit states must be separated in energy less than the band widths (typically *ca.* 0.3 μm^{-1}). The halide π-LMCT band may also include the transition to the ^1E_u state since a separate band is not resolved. Calculated energy differences between $E_u(^1E_u)$ and the components of ^3E_u ranged from 0.1 μm^{-1} for chloro complexes to 0.5 μm^{-1} for iodo complexes.

An alternative assignment of band III for *trans*-$Rh(en)_2X_2^+$, *trans*-$Rh(NH_3)_4X_2^+$, *trans*-$Pt(en)_2X_2^{2+}$ and *trans*-$Pt(NH_3)_4X_2^{2+}$ (X = Cl or Br) or band IV for *trans*-$Ir(en)_2Br_2^+$ to an intensity-enhanced LF transition is considered unlikely. Low temperature measurements on several bromo complexes in solid PVA films (see Figure 4) revealed typical charge-transfer temperature dependence, showing band sharpening and an increase in maximum absorbtivity. Vibronic LF bands are expected to decrease in total intensity as the temperature is lowered.

Two additional bands are observed in the high energy region in *trans*-$Rh(en)_2I_2^+$. The first of these, a shoulder at 4.55 μm^{-1} (band V), is assigned as the π-LMCT involving the higher energy $2b_{1g}$ ($d_{x^2-y^2}$) metal orbital. Both the energy and intensity of this band are consistent with this assignment. The second, higher energy band (band VI) is similar in energy to comparable bands observed for the other iodo complexes, and is tentatively assigned as an iodide intraligand transition from an I^- 5p orbital to either a 5d or 6s orbital, whichever is lower in energy.

The spectra obtained for *trans*-$Pt(NH_3)_4I_2^{2+}$ did not follow Beer's law, probably due to reduction of Pt(IV) to Pt(II). However the bands observed are consistent with those expected for the *trans*-$Pt(NH_3)_4I_2^{2+}$ ion and the energies are included in Table III for comparison purposes despite the complications. The absorptions due to $Pt(NH_3)_4^{2+}$, the likely Pt(II) reduction product, are very weak at energies below 4.7 μm^{-1} [39] and therefore would not affect the energies of the bands of the Pt(IV) complex. Attempts to prepare *trans*-$[Pt(en)_2I_2](ClO_4)_2$ yielded only the Pt(II)–Pt(IV) mixed valence compound $[Pt(en)_2I_2]\cdot[Pt(en)_2]$.

Trans-*Pt(CN)*$_4X_2^{2-}$ *and* trans-*Pt(NO*$_2$*)*$_4X_2^{2-}$

The spectra of the *trans*-$Pt(CN)_4X_2^{2-}$ (X = Cl or Br) anions are remarkably similar to the spectra of the *trans*-$Pt(en)_2X_2^{2+}$ or *trans*-$Pt(NH_3)_4X_2^{2+}$ (X = Cl or Br) cations. Consequently both LF and LMCT assignments are analogous. The marked similarity between the spectra of the CN^- complexes and the NH_3 or en complexes demonstrates the dominating effect the halide ligands have on the low energy excited states for these Pt(IV) complexes. Perhaps this is not too surprising since the lowest energy

excited states of $Pt(NH_3)_6^{4+}$ or $Pt(en)_3^{4+}$ and $Pt(CN)_6^{2-}$ are considerably higher than those of PtX_6^{2-} (X = Cl or Br [4].

In contrast to the cyano complexes, the nitro complexes exhibit three intense bands (bands I, II and IV) whose energies and intensities are nearly halide independent and differ from the spectral pattern of the other complexes. These bands are likely due to intraligand O → π* transitions located on the NO_2^- ligands. The free NO_2^- ligand absorbs in this energy region and bands are also observed at similar energies for the hexanitro complexes of Pt(IV) and Rh(III) [4, 41, 42]. Band III observed at 4.33 μm^{-1} in *trans*-$Pt(NO_2)_4Br_2^{2-}$ lies only 0.2 μm^{-1} higher in energy than the $^1A_{1g} \rightarrow {}^1A_{2u}$ transition in *trans*-$Pt(CN)_4Br_2^{2-}$, and therefore is assigned similarly. The analogous band in *trans*-$Pt(NO_2)_4Cl_2^{2-}$ would lie at higher energy and is probably obscured by the intense NO_2^- band at 5.1 μm^{-1} (band IV).

$M(NH_3)_5X^{n+}$ and $Pt(CN)_5X^{2-}$ Complexes

The pattern of assignments used for the D_{4h} complexes can be extended to these C_{4v} complexes. For example, the LF transitions $^1A_1 \rightarrow a^3E$ and $^1A_1 \rightarrow a^1E$ in $M(NH_3)_5X^{n+}$ are shifted *ca.* 0.4–0.5 μm^{-1} to higher energy compared to the analogous transitions in the *trans*-$M(NH_3)_4X_2^{n+}$ or *trans*-$M(en)_2X_2^{n+}$ complexes of the same metal ion. Such a shift is easily rationalized by the increase in axial ligand field on replacing a weak field X^- ligand with a stronger field NH_3 ligand. This replacement is expected to destabilize the $4a_1$ (d_{z^2}) metal orbital and stabilize the 3e (d_{xz}, d_{yz}) metal orbitals. A similar effect, though slightly larger (0.8 μm^{-1}) is observed in comparing the energies of the $^1A_{1g} \rightarrow a^1E_g$ transition in *trans*-$Pt(CN)_4Cl_2^{2-}$ (band II) and the $^1A_1 \rightarrow a^1E$ transition in $Pt(CN)_5Cl^{2-}$ (band I). In the case of $Rh(NH_3)_5I^{2+}$ and $Pt(NH_3)_5I^{3+}$ a shoulder (band II) is observed on the high energy side of the $^1A_1 \rightarrow a^1E$ LF band. These shoulders are probably analogous to the high energy LF bands discussed above for the *trans*-$Ir(en)_2X_2^+$ (X = Cl or Br) complexes. They may be assigned either to the orbitally forbidden $^1A_1 \rightarrow {}^1A_2$ transition or to spin-forbidden LF transitions, with the latter assignment being preferable on energetic grounds.

The destabilization of the $4a_1$ metal orbital is also reflected in the higher energies of LMCT bands in the C_{4v} complexes compared to the D_{4h} complexes. However, the pattern of band intensities as a function of the halide ligand is substantially the same for the two structural types and can be rationalized by similar arguments. Spin–orbit calculations lead to the same conclusions as before regarding the halide spin–orbit coupling in the π-LMCT states. The destabilization of the $4a_1$ orbital is also expected to reduce the energy difference between the LMCT excited configurations involving this orbital and the higher energy $2b_1$ ($d_{x^2-y^2}$) metal orbital. A second lower intensity LMCT band (band V) is observed for the $Ir(NH_3)_5X^{2+}$ complexes somewhat higher in energy than the $4a_1$ π-LMCT transitions. This band is assigned as the π-LMCT transitions to $2b_1$.

Finally it may be noted that both the LF and MLCT assignments given here for the $Pt(CN)_5X^{2-}$ complexes are consistent with those of Geoffroy *et al.* [23] for $Rh(CN)_5X^{3-}$ and $Ir(CN)_5X^{3-}$. Furthermore, solid film (methylmethacrylate) spectra at 23K corroborate the π-LMCT assignment for band II for $Pt(CN)_5Br^{2-}$ and $Pt(CN)_5I^{2-}$.

Trends in LF and LMCT Energies

The transition to the a^1E_g or a^1E LF state is observed for nearly all the complexes investigated here, which allows some comparisons to be made. Observed energies, together with data for related Co(III) [36], Pd(IV) [43], and $M(CN)_5X^{-3}$, M = Rh(III) and Ir(III) [23], complexes are collected in Table V. The expected increase in energy Co(III) < Rh(III) < Ir(III) and Pd(IV) < Pt(IV) is clearly observed for the a^1E_g and a^1E states. However, the energies of these states for analogous complexes of Pt(IV) and Ir(III) are nearly the same. Similarly for Pd(IV) and Rh(III). Since it is probable that electronic repulsions will increase with metal oxidation state, the similarity of energies between analogous complexes of the isoelectronic metal ions may indicate a *decrease* in LF splitting as the metal oxidation state increases. This trend, which is a reversal of behavior predicted from crystal field theory, was also noted earlier [7] for some MX_6^m halide complexes of Pt(IV) and Ir(III) and has been observed in several square-planar halide complexes [7, 39]. A decrease in LF splitting likely reflects a decrease in bonding to the more contracted *n*d orbitals of the metal ion in the higher oxidation state.

TABLE V. Energies [a] of the a^1E_g or a^1E LF States Above the Ground State.

Complex	Co(III)	Rh(III)	Ir(III)	Pd(IV)	Pt(IV)
a^1E_g States					
trans-$M(en)_2Cl_2^{n+}$	1.61[b]	2.47	2.92	2.46[c]	3.03
trans-$M(en)_2Br_2^{n+}$	1.52[b]	2.36	2.76	2.38[c]	2.70
trans-$M(en)_2I_2^{n+}$		2.17	2.53		
a^1E States					
$M(NH_3)_5Cl^{n+}$	1.87[b]	2.90	3.49		3.54
$M(NH_3)_5Br^{n+}$	1.82[b]	2.80	3.31		3.11
$M(NH_3)_5I^{n+}$	1.72[b]	2.42	2.99		2.58
$M(CN)_5Cl^{n-}$	2.56[d]	3.61[d]	4.08[d]		3.84
$M(CN)_5Br^{n-}$		3.48[d]	3.81[d]		
$M(CN)_5I^{n-}$		3.19[d]	3.64[d]		

[a] In μm^{-1}; data from Table III except as indicated. [b] Ref. 36. [c] Ref. 43. [d] Ref. 23.

Metal to ligand π bonding (back bonding) to CN^- will also be greatly reduced in complexes of metal ions with highly contracted, occupied *n*d orbitals. This is undoubtedly the case for the *trans*-$Pt(CN)_4X_2^{2-}$ complexes, and is probably responsible for the close similarity of the LF energies of these anionic complexes and the corresponding cationic *trans*-$Pt(en)_2X_2^{2+}$ or *trans*-$Pt(NH_3)_4Br_2^{2+}$, as noted in the discussion of spectral assignments. If the non-π-bonding N-donor ligands and the CN^- ligand have nearly the same σ-donor ability toward Pt(IV), then similar LF energies are expected since the π bonding will be limited to the halide ligands alone.

The bands of intermediate intensity which are dependent upon the nature of the halide were assigned as π-LMCT. The energies of these transitions as well as the energies of the more intense σ-LMCT transition follow the expected pattern predicted from metal orbital stability. However, a closer examination of the energies of corresponding π-LMCT or σ-LMCT states of analogous Rh(III) and Pt(IV) complexes shows that the energies are nearly the same. If differences in electron repulsions are small the similarity suggests nearly equal orbital stability for Rh(III) and Pt(IV). By the same argument orbitals of both of these metal ions are 0.7–1.2 μm^{-1} more stable than orbitals of Ir(III).

The energies of the σ- and π-LMCT states involving the d_{z^2} orbital in *trans*-$ML_4X_2^m$ complexes are not very sensitive to the nature of the L ligands. Some comparative data which illustrate this trend are collected in Table VI. The small energy differences in the π-LMCT or σ-LMCT states that are observed as a function of L may be rationalized partly in terms of minor differences in electron repulsions and/or solution environment. This result indicates that, insofar as LMCT to the metal d_{z^2} orbital is concerned, the X–M–X acts as a chromophoric unit (along the z axis) which is virtually independent of the equatorial ligands (in the xy plane). This feature is consonant with the observation that many photochemical reactions of these tetragonal complexes involving irradiation in the LMCT energy region lead to stereospecific labilization of the M–X bonds [20, 21].

Finally, it may be noted that energy differences between σ-LMCT and π-LMCT excited states involving the metal d_{z^2} orbital are fairly constant for a given metal ion. Similar trends have been noted for octahedral and square-planar complexes exhibiting halide or pseudohalide LMCT [4, 7, 39]. Though data are somewhat limited, the energy difference between the σ- and π-LMCT states appears to increase significantly with metal oxidation state. For example, the differences in Table VI for several Rh(III) complexes are 0.6–0.7 μm^{-1} while for the Pt(IV) complexes, and the Pd(IV) complexes also, they are in the range 1.0–1.2 μm^{-1}. A similar trend is found in comparisons among the $M(NH_3)_5X^{n+}$ and $M(CN)_5^{m-}$ complexes (Table III, together with data in ref. 23). This trend may be partly due to differences in electronic repulsions but the difference also reflects the relative σ and π X orbital stability as affected by bonding to the metal ion. Thus the difference may result from an enhancement of X → M σ bonding compared to π bonding as the metal oxidation state increases. This might be visualized in a qualitative way as a "crystal field splitting" of the σ and π orbitals of the X ligand by the charged metal ion [44].

TABLE VI. Energies [a] of Halide LMCT States in *trans*-$ML_4X_2^m$ Complexes.

L	π-LMCT[b]	σ-LMCT[c]	L	π-LMCT[b]	σ-LMCT[c]
trans-$PtL_4Cl_2^m$			*trans*-$PtL_4Br_2^m$		
Cl^-	3.82[d]	4.95[d]	Br^-	3.19[d] 3.29[d]	4.37[d]
½en	3.81	4.82	½en	3.13	4.25
NH_3	3.86	4.80	NH_3	3.16	4.24
CN^-	3.47	4.58	CN^-	2.88	4.14
			NO_2^-		4.33
trans-$IrL_4Br_2^m$			*trans*-$PdL_4Cl_2^m$		
Br^-	4.11[e]		Cl^-	2.94[e]	4.17[e]
½en	4.35		½en	2.88[f]	3.95[f]
trans-$RhL_4Cl_2^m$			*trans*-$RhL_4Br_2^m$		
Cl^-	3.92[e]		Br^-	3.01, 3.39[e]	
½en	4.13	4.86	½en	3.63	4.30
NH_3		4.81	NH_3	3.68	4.27

[a] In μm^{-1}; data from Table III except as noted. [b] $^1A_{1g} \rightarrow {}^1T_{1u}[(t_{1u}^{\pi})^5 e_g]$ for the O_h complexes or $^1A_{1g} \rightarrow {}^{1,3}E_u[(2e_u)^3(3a_{1g})]$ for the tetragonal complexes. [c] $^1A_{1g} \rightarrow {}^1T_{1u}[(t_{1u}^{\sigma})^5 e_g]$ for the O_h complexes or $^1A_{1g} \rightarrow {}^1A_{2u}[(1a_{2u})(3a_{1g})]$ in the tetragonal complexes. [d] Ref. 4 and 5. [e] Ref. 37. [f] Ref. 43.

References

1 Abstracted in part from the Ph.D. dissertation of WDB, Northern Illinois University, May 1977.
2 C. K. Jørgensen, "Absorption Spectra and Chemical Bonding in Complexes", Addison–Wesley, Reading, Mass. (1962).
3 A. B. P. Lever, "Inorganic Electronic Spectroscopy", Elsevier (1968).
4 D. L. Swihart and W. R. Mason, *Inorg. Chem.*, *9*, 1749 (1970).
5 C. K. Jørgensen, in "Advances in Chemical Physics", Vol. 5, I. Prigogine, ed., Interscience, New York, N.Y. (1963) p. 33.
6 K. A. Schroeder, *J. Chem. Phys.*, *37*, 2553 (1962).
7 C. J. Ballhausen and H. B. Gray in "Coordination Chemistry", Am. Chem. Soc. Monograph No. 168, A. E. Martell, ed., Van Nostrand–Reinhold, New York, N.Y. (1971) p. 3.
8 C. J. Ballhausen, "Introduction to Ligand Field Theory", McGraw–Hill, New York, N.Y. (1962).

9 H. H. Schmidtke, *Inorg. Chem., 5,* 1682 (1966).
10 C. K. Jørgensen, *Acta Chem. Scand., 10,* 500 (1956).
11 C. Burgess, F. R. Hartley and D. E. Rogers, *Inorg. Chim. Acta, 13,* 35 (1975).
12 (a) H. L. Bott and A. J. Poë, *J. Chem. Soc.,* 5931 (1965); (b) E. J. Bounsall and A. J. Poë, *J. Chem. Soc. A,* 286 (1966); (c) A. J. Poë and M. V. Twigg, *Can. J. Chem., 50,* 1089 (1972).
13 S. A. Johnson and F. Basolo, *Inorg. Chem., 1,* 925 (1962).
14 R. A. Bauer and F. Basolo, *Inorg. Chem., 8,* 2231 (1969).
15 C. K. Jørgensen, *Acta Chem. Scand., 10,* 518 (1956).
16 F. Basolo, J. C. Bailar, Jr. and B. R. Tarr, *J. Am. Chem. Soc., 72,* 2433 (1950).
17 A. J. Poë, *J. Chem. Soc.,* 183 (1963).
18 I. I. Chernyaev, A. V. Babkov and N. N. Zheligovskaya, *Russ. J. Inorg. Chem., 8,* 1279 (1963).
19 A. J. Poë and D. H. Vaughn, *Inorg. Chim. Acta, 2,* 159 (1968).
20 P. C. Ford, J. D. Peterson and R. E. Hintz, *Coord. Chem. Rev., 14,* 67 (1974).
21 V. Balzani and V. Carassiti, "Photochemistry of Coordination Compounds", Academic Press, New York, N.Y. (1970). Ch. 12 and pp. 308 ff.
22 M. S. Wrighton, *Topics in Current Chemistry, 65,* 37 (1976).
23 G. L. Geoffroy, M. S. Wrighton, G. S. Hammond and H. B. Gray, *Inorg. Chem., 13,* 430 (1974).
24 G. W. Bushnell, G. C. Lalor and E. A. Moelwyn-Hughes, *J. Chem. Soc. A,* 719 (1966).
25 H. H. Schmidtke, *Inorg. Syn., 12,* 245 (1970).
26 G. W. Watt and R. E. McCarley, *J. Am. Chem. Soc., 79,* 3315 (1957).
27 R. R. Rettew and R. C. Johnson, *Inorg. Chem., 4,* 1565 (1965).
28 "Gmelins Handbuch der Anorganischen Chemie", 8th ed., Vol. 68D, Verlag Chemie, Weinheim/Bergstrasse, Germany (1957) pp. 484–485.
29 I. I. Chernyaev and V. S. Orlova, *Russ. J. Inorg. Chem., 6,* 653 (1961).
30 I. B. Baranovskii, O. N. Evstaf'eva and A. V. Babaeva, *Dokl. Akad. Nauk SSSR, 163,* 642 (1965).
31 A. V. Babkov, *Dokl. Akad. Nauk SSSR, 177,* 337 (1967).
32 W. R. Mason, *Inorg. Chem., 9,* 1528 (1970).
33 W. R. Mason, *Inorg. Chem., 8,* 1756 (1969).
34 Reference 28, Vol. 68C, 1939, p. 188.
35 H. Isci and W. R. Mason, *Inorg. Chem., 14,* 905 (1975).
36 R. A. D. Wentworth and T. S. Piper, *Inorg. Chem., 4,* 709 (1965).
37 C. K. Jørgensen, *Mol. Phys., 2,* 309 (1959).
38 M. K. DeArmond and J. E. Hillis, *J. Chem. Phys., 54,* 2247 (1971).
39 W. R. Mason and H. B. Gray, *J. Am. Chem. Soc., 90,* 5721 (1968).
40 H. Yamatera, *J. Inorg. Nucl. Chem., 15,* 50 (1960).
41 H. H. Schmidtke, *Z. Physik. Chem. Neue Folge, 40,* 96 (1970).
42 K. G. Caulton and R. F. Fenske, *Inorg. Chem., 6,* 562 (1967).
43 W. R. Mason, *Inorg. Chem., 12,* 20 (1973).
44 The authors are indebted to H. B. Gray for suggesting this idea.